Contract No:

This document was prepared in conjunction with work accomplished under Contract No. 89303321CEM000080 with the U.S. Department of Energy (DOE) Office of Environmental Management (EM).

Disclaimer:

Proceedings of the ASME 14th International Pipeline Conference
IPC2022
September 26 - 30, 2022, Calgary, Alberta, Canada

[redacted]

IPC2022-86922

PROGRESS OF ASSESSMENT MODEL DEVELOPMENT FOR DETERMINING REMAINING STRENGTH OF CORRODED PIPELINES

Xian-Kui Zhu, Bruce Wiersma
Materials Technology
Savannah River National Laboratory
Aiken, South Carolina 29808, USA

ABSTRACT

A technical review is presented on corrosion assessment models for determining the remaining strength of pipelines containing metal loss or corrosion defects. The review is first given to burst prediction models for defect-free pipes, including the strength and flow solutions of burst pressure and their experimental validations. For determining more accurate burst pressure, thick-wall theoretical solutions and machine learning models are discussed and compared with full-scale burst test data that cover a wide range of pipeline grades up to X120.

The review then goes to available corrosion assessment models that are categorized into three generations in terms of the reference stress. The 1st, 2nd, and 3rd generations corresponds the flow stress, UTS and both UTS and strain hardening rate. Seventeen corrosion models are evaluated in comparison with full-scale burst data for a wide range of pipeline steels from low to high grades. The central attention focuses on validating two new 3rd-generation models that can determine more accurate remaining strength for corroded thin-wall pipes. As the 4th-generation, typical thick-wall corrosion assessment models and machine learning models are introduced for predicting more accurate results for corroded thick-wall pipes.

After that, progresses of corrosion model development are discussed, including PRCI corrosion projects, constraint effect, bulging factor and defect width effect. Finally, major technical challenges in development of corrosion assessment models are discussed as regard to full-scale experiments, numerical simulations, material failure criteria and real corrosion defects.

KEYWORDS: pipeline, corrosion defect, remaining strength, defect assessment model

1. Introduction

The pipeline system is an important infrastructure in the energy sector that has been used as an economic and safe vehicle in transportation of a large volume of crude oil or natural gas over long distances to meet the increasing demands of energy. The line pipes are made of carbon steels, and most pipelines are buried underground per the regulation requirements. Because of underground water or sour soils, steel pipes are susceptible to external corrosion attack that threatens the pipeline integrity. The U.S. Department of Transportation (DOT) [1] has collected pipeline incident reports since 1970 and updates data every year. Dai et al. [2] presented a statistical analysis on recent significant incidents for crude oil and natural gas pipelines, and showed that corrosion is one of three major failure causes for both the oil and gas pipelines. As such, corrosion assessment is critical for pipeline operators to manage the asset integrity for buried pipelines, particularly for unprotected pipelines [3].

For determining the maximum loading capacity of pressure vessels, many empirical, analytical or numerical methods [4] have been developed for defect-free cylinders subject to internal pressure. Christopher et al. [5] evaluated a set of available burst pressure prediction models for both thin-wall and thick-wall pressure vessels. Law and Bowie [6] assessed the burst pressure prediction models for high-strength line pipes. More recently, Zhu and Leis [7] evaluated a series of burst pressure prediction models for a variety of pipeline steels in terms of the strength theories and the plastic flow theories. The most accurate model was identified for defect-free line pipes.

The natural gas industry began work to investigate the threat posed by corrosion in the late 1960s [8], with a view to quantify when a reinforcement or replacement of corroded pipes was required. Experimental data of full-scale tests on pipe segments

This work was produced by Battelle Savannah River Alliance, LLC under Contract No. 89303321CEM000080 with the U.S. Department of Energy. Publisher acknowledges the U.S. Government license to provide public access under the DOE Public Access Plan (http://energy.gov/downloads/doe-public-access-plan).

removed from service lines were trended in terms of burst pressure as a function of the length and depth of metal-loss defects [8]. The trending function was originated in the NG-18 equations [9-10] that were developed at Battelle in the early 1970s for determining fracture failure of pipelines containing cracks. Based on the NG-18 equation for collapse-controlled failure, the oil and gas industry developed an empirical corrosion assessment code, and ASME published the first edition of B31G manual for determining the remaining strength of corroded pipelines in 1984, the Modified B31G in 1989, and the current edition of B31G-2009 [11].

With the advances of steel making technology, both strength and toughness of modern pipeline steels have significantly improved, and many high-strength pipeline grades, such as X70 and X80, have been utilized today. Accordingly, numerous effects were made over the past decades, and many improved corrosion assessment methods [12] were developed for better managing the high-strength pipelines. Among them, the ultimate tensile stress (UTS)-based method can determine more accurate burst pressure of corroded line pipes, and thus has been accepted by Standards BS 7910 [13] and API 579 [14] for a general engineering critical analysis (ECA) or fitness for service (FFS) assessment of pressure vessels. However, ASME B31G and Mod B31G remain in use today in the pipeline industry, even though those methods are well known to be (overly) conservative.

Recently, Zhu [15] summarized primary available corrosion assessment methods for metal-loss defects in pipelines and discussed some practical challenges facing the oil and gas industry. Zhu [16] discussed the numerical approaches used to predict burst pressure of line pipes with metal-loss defects. Leis et al. [17] presented their numerical results to minimize the B31G model uncertainty in the corrosion assessment. Zhou and Huang [18] assessed the model errors of corrosion models. Amaya-Gomez et al. [19] assessed the reliability of corrosion methods, and Bhardwaj et al. [20] quantified the uncertainty of burst pressure models of corroded pipelines. However, those publications have limited discussions on strain hardening effect, and the machine learning application is not addressed yet.

So motivated, this paper performs a comparative study on remaining strength assessment models for corroded pipelines. A brief review of burst prediction models is first given to defect-free pipes and then to corroded pipes. For better understanding the development of corrosion models, typical burst models are categorized and critically evaluated in comparison to full-scale burst test data, with a focus on validating the newly proposed corrosion models. Recent progresses are also presented, including those from PRCI corrosion projects, theoretical solutions for thick-wall pipes, and machine learning models. Finally, major technical challenges are discussed for further improving the corrosion assessment models.

2. Burst pressure models for defect-free pipes

The burst pressure prediction for defect-free pipes is the basis for developing corrosion models for assessing line pipes containing corrosion or metal-loss defects [4], where the reference stress of corrosion model is defined by the burst pressure of defect-free pipes. This section briefly reviews the strength and flow models of burst pressure for thin-wall defect-free pipes, new strength theories for thick-wall defect-free pipes and machine learning models.

2.1. Strength models of burst pressure

For a large diameter, thin-wall defect-free pipe, four strength models [4] of burst pressure were obtained in terms of the UTS and the Tresca, von Mises and Zhu-Leis criteria as well as the flow stress criterion [10].

1). Tresca strength solution:

$$P_0 = \frac{2t}{D}\sigma_{uts} \tag{1}$$

2). von Mises strength solution:

$$P_{M0} = \frac{4t}{\sqrt{3}D}\sigma_{uts} \tag{2}$$

3). Zhu-Leis strength solution:

$$P_{ZL0} = \frac{1}{2}\left(1+\frac{2}{\sqrt{3}}\right)\frac{2t}{D}\sigma_{uts} \tag{3}$$

4). Flow stress-based failure solution:

$$P_{f0} = \frac{2t}{D}\sigma_{flow} \tag{4}$$

where D ($\bar{D}$) is the outside (mean) diameter, and t is the wall thickness. The flow stress $\sigma_{flow} = (\sigma_{ys}+\sigma_{uts})/2$, with σ_{ys} the yield stress (YS) and σ_{uts} the UTS. Zhu-Leis strength solution in Eq. (3) was determined using a new multi-axial, average shear stress strength theory developed by Zhu and Leis [21-22]. Equations (1) to (3) show that the Zhu-Leis strength solution is equivalent to the average of Tresca and Mises strength solutions.

To evaluate the accuracy of four strength models in Eqs (1) to (4), experimental data of burst pressure (P_b) for more than 100 full-scale tests of thin-wall cylindrical pressure vessels made of carbon steels were used to compare with the burst pressure predictions from the four strength criteria, as shown in Fig. 1. All materials used in the experiments are ductile steels with a wide range of strain hardening exponent n from 0.02 to 0.18 that covers low to high-strength pipeline steels from Gr B to X120.

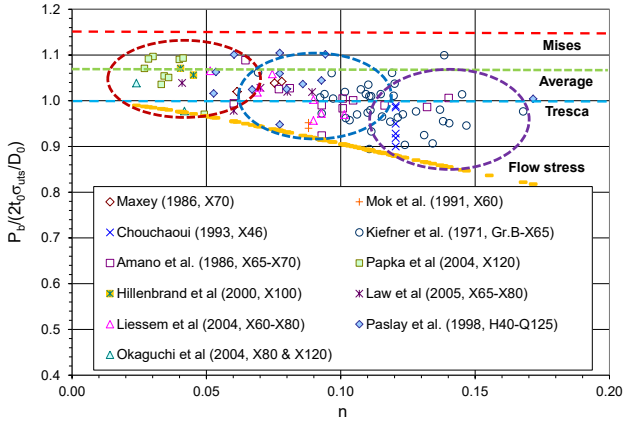

Fig. 1. Comparison of experimental data of burst pressure and predictions by von Mises, Zhu-Leis, Tresca, and flow stress criteria for various pipeline steels [4]

Experimental details and References cited in Fig. 1 were described by Zhu and Leis [21]. All points in the figure are experimental data, and all lines are burst pressure predictions. As shown in Fig. 1, three circles contain three groups of test data. The purple, blue and red circles represent test data of burst pressure for low, intermediate, and high strength carbon steels, respectively. Four dash lines in red, green, blue, and yellow denote the burst pressure predictions, respectively by the von Mises, Zhu-Leis, Tresca, and flow stress criteria. This figure shows that (1) von Mises strength criterion overestimates burst pressure for all steels, (2) Zhu-Leis strength criterion is good for high-strength steels but overestimated for low-strength steels, (3) Tresca strength criterion adequately predicts burst pressure for intermediate-strength steels, and (4) the flow stress criterion predicts the most conservative results for all steels.

Also evident in Fig. 1, experimental data of burst pressure have a linear trend with the strain hardening exponent n, and the normalized burst pressure decreases with the increasing strain hardening rate. Except for the flow stress criterion, the other three conventional strength criteria do not consider the effect of strain hardening rate on burst pressure. To improve these strength solutions, the flow theories of plasticity [4] was recommended for use to develop more accurate burst pressure solutions in reference to two material parameters.

2.2. Flow models of burst pressure

The Tresca theory and von Mises theory are two classic theories of plasticity developed for describing the nonlinear plastic deformation in a metal during loading. They can determine two bound solutions of burst pressure for the same pipe. To predict more accurate burst failure, Zhu and Leis [21-22] introduced a new concept of "average shear stress", and developed an associated multi-axial flow theory of plasticity, i.e. average shear stress flow theory that was often referred to as Zhu-Leis flow theory in public literature. For a power-law hardening material, the new flow theory determined a new flow solution of burst pressure. Accordingly, three flow solutions of burst pressure were determined for thin wall, defect-free pipes in terms of Tresca, Zhu-Leis and von Mises flow theories as:

$$P_T = \left(\frac{1}{2}\right)^{n+1} \frac{4t}{D} \sigma_{uts} \tag{5}$$

$$P_A = \left(\frac{2+\sqrt{3}}{4\sqrt{3}}\right)^{n+1} \frac{4t}{D} \sigma_{uts} \tag{6}$$

$$P_M = \left(\frac{1}{\sqrt{3}}\right)^{n+1} \frac{4t}{D} \sigma_{uts} \tag{7}$$

where n is the strain hardening exponent and can be measured from a tensile test or estimated from the Y/T ratio [21, 23].

The experimental data of burst pressure shown in Fig. 1 are reused here to assess and validate the flow theories. Figure 2 compares the experimental data with Tresca flow solution in Eq. (5), Zhu-Leis flow solution in Eq. (6) and von Mises flow solution in Eq. (7). This figure shows that (1) all test data and predictions of burst pressure are functions of strain hardening rate in a similar trend, (2) von Mises flow solution gives an upper bound prediction, (3) Tresca flow solution gives a lower bound prediction, and (4) Zhu-Leis flow solution is a better prediction that matches well with the burst data on average. Thus, those experiments validate Zhu-Leis flow theory and the associate flow solution of burst pressure for thin-wall, defect-free pipes.

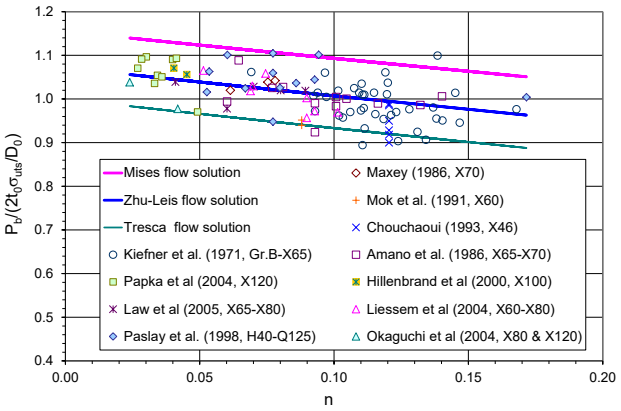

Fig. 2. Comparison of three flow solutions and experimental data for various carbon steels [21]

Using other full-scale test data and the statistical analysis, Seghier et al. [24] confirmed that the average shear stress yield criterion is the best plastic flow criterion to predict burst pressure of intact pipes for different steel grades ranging from X46 to X100. Likewise, Zimmermann et al [25-26], Zhou and Huang [27] and Bony et al. [28] among others assessed the available burst prediction models and concluded that Zhu-Leis flow solution is the most accurate burst pressure prediction model for thin-wall pipes. Thus, Zhu-Leis flow theory [21] not only fills in the technical gap between Tresca and von Mises flow theories, but also determines a more accurate burst pressure solution.

2.3. Burst pressure models for thick-wall pipes

The Zhu-Leis flow solution discussed above is accurate only for thin-wall pipes with D/t>40 and approximate for D/t≥20. In practice, there are many heavy-wall line pipes with wall thickness large than 20 mm or 40 mm [29], leading to D/t<20 or D/t<10. In this case, all thin-wall theories fail. Thus, thick-wall solutions of burst pressure are desired and must be explored.

For this purpose, recently Zhu et al. [30] introduced a yield criterion-based, two-parameter flow stress:

$$\sigma_f = \left(\frac{K}{2}\right)^n \sigma_{uts} \tag{8}$$

where K is a constant that is related to the yield criterion:

$$K = \begin{cases} 1, & \text{for Tresca yield criterion} \\ \frac{2}{\sqrt{3}}, & \text{for von Mises yield criterion} \\ \frac{1}{2} + \frac{1}{\sqrt{3}}, & \text{for Zhu-Leis yield criterion} \end{cases} \tag{9}$$

With this two-parameter flow stress, the corresponding new strength theories were developed by Zhu et al. [30], and then burst pressure solutions were obtained for thick-wall cylinders subject to internal pressure:

$$P_b = 2\left(\frac{K}{2}\right)^{n+1}\sigma_{uts}ln\left(\frac{D_0}{D_i}\right) \quad (10)$$

where D_0 (D_i) is the outside (inside) diameter of the pipe, and K takes the value in Eq. (9). Equation (10) is the burst pressure solutions for thick-wall pipes corresponding to Tresca, von Mises and Zhu-Leis criteria. From Tayler series, one has $\ln(D_0/D_i) = 2t/D_0 + 0.5(2t/D_0)^2$. The error of the second term is less than 2.5% if $D_0/t>40$ or 5% if $D_0/t>20$, but the error will be larger than 10% if $D_0/t\leq 10$ for thick-wall pipes. As a result, the thin-wall burst solution is "accurate" only for D/t>40.

Figure 3 compares the Zhu-Leis burst pressure solutions predicted from Eq. (6) and Eq. (10) with the full-scale burst data (as shown in Fig. 1 with limited burst data for thick-wall pipes) as a function of D/t. From this figure, it is observed that:

(1) The newly proposed Zhu-Leis solution of burst pressure for thick walls in Eq. (10) is very accurate and closely matches the burst pressure data for all pipes with a wide range of D/t ratios, including thin to thick walls.

(2) For thin-wall pipes with $D/t > 20$, all burst pressures are near to or less than 5,000 psi (34.47 MPa). The Zhu-Leis burst pressure solution for the thin-wall theory is very close to that for the thick-wall theory.

(3) For intermediate to thick-wall pipes with $D/t < 20$, all burst pressures are larger than 5,000 psi (34.47 MPa). The mean diameter (MD)-based Zhu-Leis solution for thin-wall pipes is either comparable or nearly identical to Zhu-Leis burst pressure solution for thick-wall pipes.

(4) In contrast, the OD-based Zhu-Leis solutions for thin-wall pipes is significantly lower than those for the thick-wall pipes with D/t<10. *As a result, the MD-based rather than OD-based Zhu-Leis solution should be used generally.*

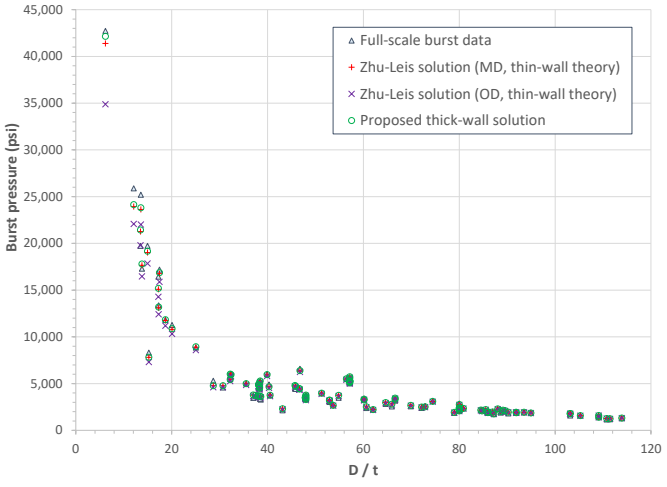

Figure 3. Comparison of predicted and measured burst pressures in the function of D/t (30)

2.4. Machine learning models of burst pressure

Recently, Zhu et al. [31] applied the state-of-the-art machine learning technology to model the burst strength of defect-free pipes in reference to a wide range of D/t ratios and steel grades. Using the full-scale burst dataset shown in Fig. 1, three artificial neural network (ANN) architectures were created, and three ANN models of burst pressure were determined. ANN model 1 has one input variable and one hidden layer, ANN model 2 has three input variables and one hidden layer, ANN model 3 has three input variables and two hidden layers, and all three ANN models have one output variable.

Figure 4 shows the architecture of ANN model 2, where three input variables are X1 = n, X2 = UTS, and X3 = D/t, and the output variable Y = burst pressure. For each ANN model, two activation functions were used to connect neurons in different layers by use of wights and bias at each unknown unit. The activation functions coupled with specific algorithms were used to train and learn from the training dataset until the model performance is satisfied in comparison to the validation dataset. Once the ANN model is fully built, it can be used to predict burst pressure for pipes with different diameters and wall thicknesses in any pipeline steel.

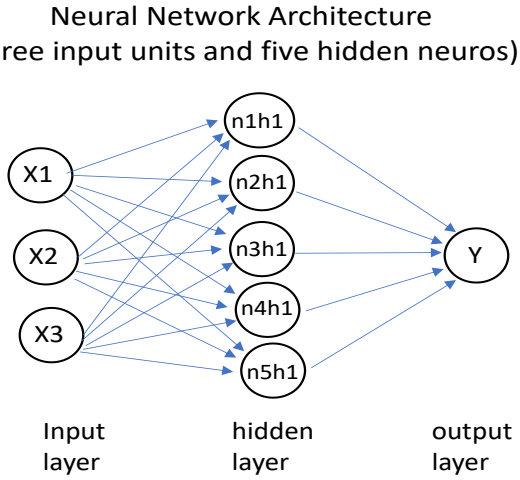

Figure 4. Architecture of ANN model 2

Figure 5 compares the model predicted burst strengths with the measured burst pressure data for the full-scale tests in consideration, where the model predictions include those predicted by the three ANN models, the linear regression result, and the Zhu-Leis solution for thick-wall pipes. As evident in this figure, all model predictions are nearly identical to the burst data when the measured burst strength is less than 15 ksi (103.42 MPa), while some deviations are observed when the measured burst pressure is large than 15 ksi (103.42 MPa). For the latter case, the model predictions from ANN model 2 and model 3 are more accurate than other models. Due to the simple architecture, ANN model 2 is recommended as the best machine learning model for predicting burst strength of defect-free, thin-wall or thick-wall line pipes.

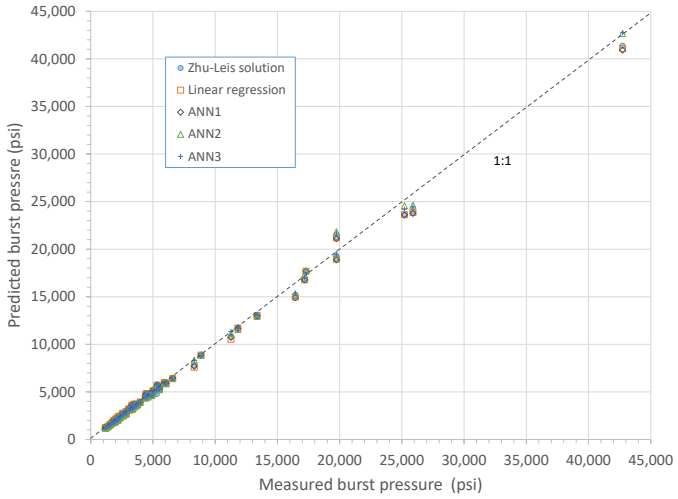

Figure 5. Variation of predicted burst strength with measured burst strength for all full-scale tests [31]

3. Corrosion assessment models

Corrosion defects formed in ageing pipelines can be very complicated in size, shape, location and orientation. Only axially oriented, isolated metal-loss defects in line pipes subject to internal pressure are considered in this work. Other anomalies and loading conditions will not be considered.

A general expression of burst failure stress or pressure of a corrosion defect can be written as:

$$S_f = S_R \times f(\text{defect geometry}) \quad (11)$$

$$P_b = S_R\, 2t/D \times f(\text{defect geometry}) \quad (12)$$

where S_f denotes the burst hoop stress, P_b is the burst pressure, S_R is a reference stress, and f is a function of defect geometry (depth d, length L and width W). In many cases, defect width has small effect, and f can be simplified as $f(d/t, L/\sqrt{(Dt)})$. Absent a defect, Eq. (11) must predict the failure stress of defect-free pipe, and thus S_R is equal to the failure stress of defect-free pipes. Note that Eq. (12) is consistent with the notation used in API 579 [14] for Level-1 defect criterion.

Based on different definitions of the reference stress, available corrosion models can be categorized into three big generations as reviewed below. The newest fourth generation is ongoing in developing.

3.1. The first-generation models (1960s – 1970s)

The first-generation models are empirical and developed in the 1960s to 1970s with the reference stress S_R=the flow stress.

3.1.1. ASME B31G

Based on full-scale test data obtained in the early 1970s for pipeline steels up to X65, Maxey et al. [10-11] developed a set of semi-empirical equations (i.e., NG-18 equations) to estimate the burst pressure of line pipes with cracks. Based on NG-18 equation for collapse-controlled failure, a corrosion assessment model B31G was developed by ASME, and the first edition was published in 1984. For a short defect, corrosion area was assumed to be parabolic in shape with a curved bottom, and the burst pressure of the corroded pipeline is estimated by:

$$p_b = \frac{2t\sigma_f}{D}\left[\frac{1-(2/3)(d/t)}{1-(2/3)(d/t)/M}\right], \quad \text{for } L \le \sqrt{20Dt} \quad (13)$$

where the defect depth is limited within 80% of t, or d/t ≤ 0.8.

For a long corrosion defect, corrosion area was assumed to have a rectangular shape with flat bottom, and Eq. (10) becomes:

$$p_b = \frac{2t\sigma_f}{D}\left[1-\frac{d}{t}\right], \quad \text{for } L > \sqrt{20Dt} \quad (14)$$

In both equations above, the flow stress $\sigma_f = 1.1$ SMYS, where SMYS is the specified minimum yield stress defined in API 5L [32], and M is a Folia's bulging factor [33] expressed as:

$$M = \sqrt{1+0.8\left(\frac{L}{\sqrt{Dt}}\right)^2} \quad (15)$$

ASME B31G model was calibrated with the vintage pipeline grades up to X65, and thus may be inadequate to use for modern pipeline steels like X80 or X100.

3.1.2. Mod B31G (0.85 dL)

Practical applications showed that ASME B31G model can be overly conservative [34], and thus the modified B31G was proposed in 1989 by Kiefner and Vieth [35-36] in the associated software RSTRENG as follows:

$$p_b = \frac{2t\sigma_f}{D}\left[\frac{1-0.85(d/t)}{1-0.85(d/t)/M}\right] \quad (16)$$

where the defect depth is limited within 80% of t or d/t ≤ 0.8, the flow stress was redefined as $\sigma_f = SMYS + 69\ (MPa)$, and the bulging factor M was replaced by:

$$M = \sqrt{1+0.6275\left(\frac{L}{\sqrt{Dt}}\right)^2 - 0.003375\left(\frac{L}{\sqrt{Dt}}\right)^4}, \quad \text{if } L \le \sqrt{50Dt} \quad (17a)$$

$$M = 3.3 + 0.032\left(\frac{L}{\sqrt{Dt}}\right)^2, \quad \text{if } L > \sqrt{50Dt} \quad (17b)$$

Note that 1) the actual yield stress was used in the original NG-18 equations, 2) the SMYS makes B31G and Mod B31G more convenient and conservative for practical applications, 3) replacement of 2/3 factor in B31G with the 0.85 factor in Mod B31G reduces the model conservatism. The Mod B31G model was accepted in the newer edition of ASME B31G-2009 [11] and in Level-1 procedure of API 579-2016 [14]. Ma et al. [37] compared different versions of B31G in details.

3.1.3. PRCI RSTRENG (effective area model)

For better approximating a real corrosion area with river bottom profiles, an effective area method was proposed in 1989 by Kiefner and Vieth [35] to estimate the remaining strength:

$$P_b = \frac{2t\sigma_f}{D}\left[\frac{1-A_d/A_0}{1-A_d/A_0 M}\right] \quad (18)$$

where the flow stress and the bulging factor are the same as defined in Mod B31G, A_d denotes the effective area of a complex

corrosion defect profile, and A_0=tL is the axial cross-section area. This model allows to determine more accurate corroded area using the discrete approach, and thus to determine more accurate burst pressure of the real corrosion defect. A personal-computer code called RSTRENG [35] was developed by Pipeline Research Council International (PRCI) for predicting more accurate burst pressure for corroded pipes. This effective area model was adopted in Level-2 procedure of B31G [11] and API 579 [14].

For a machined rectangular defect with a uniform depth, Eq. (18) becomes:

$$P_b = \frac{2t\sigma_f}{D}\left[\frac{1-(d/t)}{1-(d/t)/M}\right] \quad (19)$$

If a corrosion defect is long enough, 1/M approaches zero and Eq. (19) reduces to Eq. (14). In 1992, Richie and Last [38] adapted Eq. (19) as a corrosion defect acceptance criterion, i.e., Shell-92 model with the flow stress $\sigma_f = 0.9\sigma_{uts}$ and defect depth d/t≤0.85. The Shell-92 model first used the UTS.

3.1.4. CSA Z662

Based on Eq. (19) and the Shell-92 model, Canadian Standards Association (CSA) developed their corrosion assessment code – CSA Z662 [39] to predict burst pressure by:

$$P_b = \frac{2t\sigma_f}{D}\left[\frac{1-(d_{ave}/t)}{1-(d_{ave}/t)/M}\right] \quad (20)$$

where d_{ave} is the average defect depth, the bulging factor M is the same as Eq. (17), and the flow stress is defined as:

$$\sigma_f = \begin{cases} 1.15\sigma_{ys}, & \text{SMYS}\leq 241 \text{ MPa (or 35 ksi)} \\ 0.9\sigma_{uts}, & \text{SMYS}>241 \text{ MPa (or 35 ksi)} \end{cases} \quad (21)$$

3.1.5. Comparison of the first-generation models

Figures 6 and 7 compare the first-generation (1st-G) models discussed above for a fixed uniform defect with depth of d/t=0.5 and for two lower strength steels X52 and GrB, where the x-axis denotes the normalized defect length, and the y-axis denotes the normalized burst pressure with P_b the model predicted burst pressure and P_0 the Tresca strength solution in Eq. (1). In those figures, *the 1st-G models include ASME B31G, Mod B31G, RSTRENG, Shell-92 and CSA Z662 criteria*. The material properties were assumed to be SMYS and specified minimum tensile stress (SMTS), see API 5L [32].

For X52, Fig. 6 shows that the Mod B31G model predicts the highest burst pressure for all given defect lengths; the CSA Z662 and Shell-92 are identical with predictions slightly lower than the RSTRENG results; and ASME B31G predicts a comparable result to Mod B31G for a short corrosion defect, but the lowest result for a long corrosion defect.

For GrB, Fig. 7 shows that the Shell-92 model predicts the highest results of burst pressure over the given defect length, and followed in order are Mod B31G, RSTRENG, and CSA Z662 models. ASME B31G model may predict a comparable result to RSTRENG for a short corrosion defect, but the lowest result for a long corrosion defect.

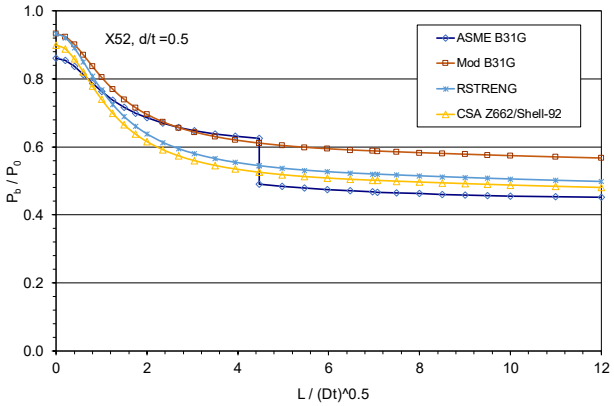

Fig. 6. Comparison of the 1st-G corrosion models for X52

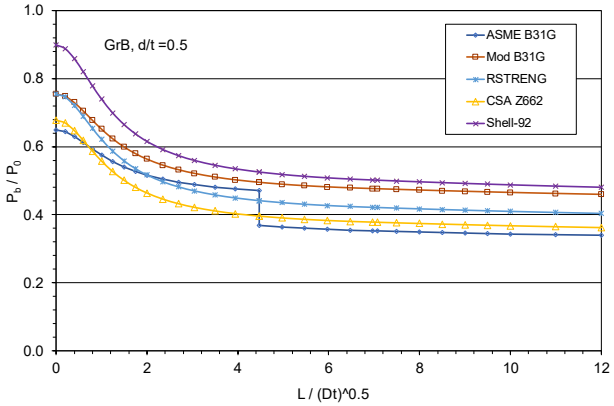

Fig. 7. Comparison of the 1st-G corrosion models for GrB

3.2. The second-generation models (1990s-2000s)

The second-generation models are numerical ones that were developed in the 1990s to 2000s with S_R = UTS.

3.2.1. LPC model

Based on a burst test database and a large amount of elastic-plastic FEA results for X65 corroded pipes, Fu et al. [40-41] at British Gas in 1995 developed a line pipe corrosion (LPC) criterion for determining burst pressure for corrode pipes:

$$P_b = \frac{2t\sigma_{uts}}{D-t}\left[\frac{1-d/t}{1-d/Qt}\right] \quad (22)$$

where σ_{uts} is the UTS of pipeline steels, and the parameter Q is a curve-fit bulging factor from the FEA results as:

$$Q = \sqrt{1+0.31\left(\frac{L}{\sqrt{Dt}}\right)^2} \quad (23)$$

The LPC criterion was adopted into DNV RP-F-101 [42] in 1999 with S_R=0.9UTS and statistical factors, and then adopted in BS7910-1999 [13] with $S_R=(\sigma_{ys}+\sigma_{uts})/2$.

3.2.2. PCORRC model

In parallel to the development of the LPC model, Leis et al. [43-44] at Battelle developed the PCORRC model:

$$P_b = \frac{2t\sigma_{uts}}{D}\left[1-\frac{d}{t}\left(1-exp(-0.157\frac{L}{\sqrt{D(t-d)/2}})\right)\right] \quad (24)$$

For a very long metal-loss defect, Eqs (22) and (24) reduce to the simple equation:

$$p_b = \frac{2t\sigma_{uts}}{D}\left[1-\frac{d}{t}\right] \quad (25)$$

Thus, LPC and PCORRC criteria are identical to each other for long corrosion defects. If a defect is absent, Eq. (25) reduce to Eq. (1), i.e., the Tresca strength solution for defect-free pipes. This implies that both LPC and PCORRC models have the basis of the Tresca criterion with one single material parameter.

3.2.3. Choi limit load

In 2003, Choi et al. [45] carried out a series of full-scale tests on machined metal-loss defects for X65 pipeline steel and performed the detailed 3D elastic-plastic FEA calculations on the defects, where all axial defects were assumed to be elliptically curved. By trending the FEA outcomes, they obtained the following limit load:

$$P_b = \begin{cases} 0.9\sigma_{uts}\frac{2t}{D_i}\left[C_0 + C_1\left(\frac{L}{\sqrt{Rt}}\right) + C_2\left(\frac{L}{\sqrt{Rt}}\right)^2\right], & \text{for } \left(\frac{L}{\sqrt{Rt}}\right) < 6 \\ \sigma_{uts}\frac{2t}{D_i}\left[C_3 + C_4\left(\frac{L}{\sqrt{Rt}}\right)\right], & \text{for } \left(\frac{L}{\sqrt{Rt}}\right) \geq 6 \end{cases} \quad (26)$$

where D_i is the inside diameter of the pipe, R is the mean radius, and C_0, C_1, C_2, C_3, C_4 are functions of d/t. Absent a defect, Eq. (26) reduces to $P_b=0.9\sigma_{uts}\times 2t/D_i$ for defect-free pipes. And thus the limit load in Eq. (26) may be conservative for some steels.

3.2.4. Recalibrated PCORRC model

Recently, based on full-scale test data and a set of 3D FEA calculations for X70 corroded pipes, Yeom et al. [46] in 2015 recalibrated the PCORRC model:

$$p_b = 0.9\sigma_{uts}\frac{2t}{D}\times\left(1-\frac{d}{t}\left(1-exp\left(-0.224\frac{L}{\sqrt{D(t-d)/2}}\right)\right)\right) \quad (27)$$

Absent a defect, again, Eq. (27) reduces to $P_b=0.9\sigma_{uts}\times(2t/D)$ for defect-free pipes. This model may be also conservative.

3.2.5. Comparison of the second-generation models

Figure 8 compares the second-generation (2nd-G) models discussed above for a fixed uniform defect depth of d/t=0.5 and for a moderate strength steel X65, where the material properties were assumed to be the SMYS and SMTS. In this figure, *the 2nd-G models include LPC, BS7910, PCORRC, Limit load by Choie (2003), and Reformulated PCORRC by Yeom (2015).* For comparison, RSTRENG and CSA Z662 are also included in Fig. 8. This figure shows that 1) LPC and PCORRC predict comparable results, 2) BS7910 and RSTRENG predict similar results that are lower than the LPC predictions, 3) CSA Z662 and Yeom (2015) predict comparable results that are lower than RSTRENG predictions, and 4) Choie (2003) and Yeom (2015) are comparable for short defects, and become almost identical to be the lower bound for long defects.

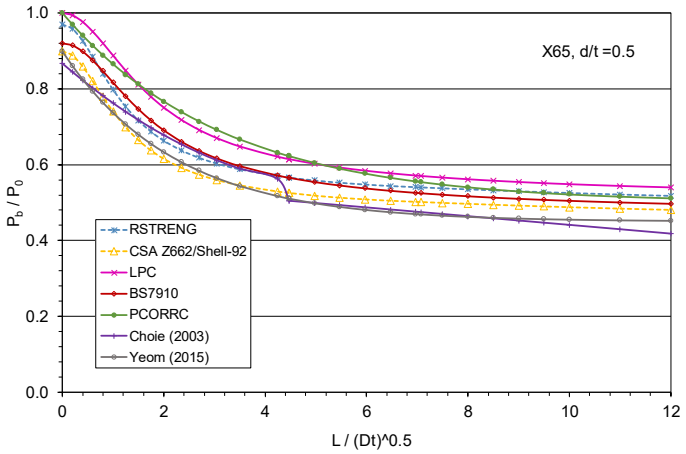

Fig. 8. Comparison of the 2nd-G corrosion models for X65

3.3. The third-generation models (2000 to 2020)

The third-generation models to be discussed below utilize a two-parameter reference stress $S_R=f$(UTS, n) that is defined from the flow theory for defect-free pipes.

3.3.1. Mises flow model coupling with PCORRC

Since the 2000s, extensive experimental and numerical studies of corroded pipes have been conducted [47-55], with a focus on the high-strength pipeline grades X70, X80 and X100. For those high-grade steels, plastic deformation local to a defect is significant at collapse due to strain hardening. In order to quantify the effect of strain hardening, Zhu and Leis [23] started to utilize the von Mises flow theory to characterize the plastic collapse of line pipes. Using the reference stress S_R from Eq. (7) and the defect geometric term of the PCORRC in Eq. (24), a modified PCORRC was obtained:

$$p_d = \frac{4}{\left(\sqrt{3}\right)^{1+0.239\left(\frac{1}{Y/T}-1\right)^{0.596}}}\frac{t}{D}\sigma_{uts}\times\left(1-\frac{d}{t}\left(1-\exp\left(-0.157\frac{L}{\sqrt{D(t-d)/2}}\right)\right)\right) \quad (28)$$

This is the first 3rd-G model that helped us understand the effect of the UTS and YS on the collapse of a defect in carbon steels. Because of non-conservatism in von Mises solution, the Zhu-2005 model in Eq. (28) may overestimate burst pressure.

3.3.2. Mises flow model coupling with reformulated PCORRC

In 2013, Ma et al. [56] also adopted the von Mises flow strength as the reference stress S_R and coupled it with the geometric term of PCORRC. After recalibration for various machined defects in X70 and X80 pipes, these authors reformulated PCORRC model for predicting the burst pressure:

$$p_d = \frac{4}{\left(\sqrt{3}\right)^{1+n}}\frac{t}{D}\sigma_{uts}\times\left(1-\frac{d}{t}\left(1-0.7501\exp\left(\frac{-0.4174L}{\sqrt{Dt}}\right)\left(1-\frac{d}{t}\right)^{-0.1151}\right)\right) \quad (29)$$

Comparison of Eqs (29) and (24) shows the geometric term in Eq. (29) is quite different from that in the PCORRC model.

3.3.3. Zhu-Leis flow model coupling with PCORRC

In order to improve the Mod PCORRC in Eq. (28) for a corroded pipeline, Zhu [57] in 2018 obtained another M-PCORRC by using the Zhu-Leis flow solution and the geometric term of PCORRC. This M-PCORRC is expressed as:

$$p_b = \left(\frac{2+\sqrt{3}}{4\sqrt{3}}\right)^{n+1} \frac{4t\sigma_{uts}}{\bar{D}} \times \left(1 - \frac{d}{t}\left(1 - exp\left(-\frac{0.157L}{\sqrt{D(t-d)/2}}\right)\right)\right) \quad (30)$$

3.3.4. Zhu-Leis flow model coupling with LPC

Similarly, using the Zhu-Leis flow solution and the geometric term of LPC, the following Mod LPC model [58] was obtained in 2021 for predicting burst pressure of corroded pipe:

$$p_b = \left(\frac{2+\sqrt{3}}{4\sqrt{3}}\right)^{n+1} \frac{4t\sigma_{uts}}{\bar{D}} \left[\frac{1-d/t}{1-d/Qt}\right] \quad (31)$$

3.3.5. Tresca flow model coupling with ASME B31.G

Recently, Abdelghani et al. [59] adopted the Tresca flow strength as S_R and coupled with the geometric term of ASME B31.G in Eq. (19). Using their FEA results, the bulging factor was recalibrated. As such, they reformulated B31G model for predicting the burst pressure of a corroded pipeline:

$$P_b = \left(\frac{1}{2}\right)^n \frac{2t\sigma_{uts}}{D} \frac{1-d/t}{1-d/tM} \quad (32)$$

where the bulging factor was recalibrated as:

$$M = \sqrt{1 + 0.45\left(\frac{L}{\sqrt{Dt}}\right)^2 + 0.050625\left(\frac{L}{\sqrt{Dt}}\right)^4} \quad (33)$$

3.3.6. Analytic model for long corrosion defects

For long corrosion defects, both LPC and PCORRC models reduce to Eq. (25) that is the Tresca strength solution coupling with a geometric factor of (1-d/t) due to a flat defect. In a similar way, Zhu [53] simply extended the plastic flow solutions in Eqs (5) to (7) for defect-free pipes to a long corrosion defect (L>D), and obtained the burst pressure as:

$$P_T = \left(\frac{K}{2}\right)^{n+1} \frac{4t\sigma_{uts}}{\bar{D}} \left[1 - \frac{d}{t}\right] \quad (34)$$

where K takes the value in Eq. (9) for the Tresca, von Mises and Zhu-Leis criteria. Using full-scale burst data [49], Zhu [53] confirmed that the Zhu-Leis solution in Eq. (34) is a better prediction of burst pressure for long corrosion defects. Thus, Eq. (34) is a 3rd-G corrosion model for a very long defect.

3.3.7. A new polynomial model

In reference to the Zhu-Leis flow solution in Eq. (34) for a long defect, Zhu [16] obtained a new polynomial corrosion model for predicting more accurate burst pressure as:

$$P_b = \left(\frac{2+\sqrt{3}}{4\sqrt{3}}\right)^{n+1} \frac{4t\sigma_{uts}}{D} \left[1 - \frac{d}{t}\left(1 - 1/\left(1 + 0.1385\frac{L}{\sqrt{Dt}} + 0.1357\left(\frac{L}{\sqrt{Dt}}\right)^2\right)\right)\right] \quad (35)$$

Note that the defect geometric function in Eq. (35) contains a polynomial and is easy for engineers to understand and use.

3.3.8. Comparison of the third-generation models

Figure 9 compares the third-generation (3rd-G) models discussed above for a fixed uniform defect depth of d/t=0.5 and for a high strength steel X70, where the material properties were assumed to be the SMYS and SMTS. In this figure, *the 3rd-G models include the first Mod PCORRC model by Zhu-2005, the reformulated PCORRC model by Ma-2013, the new corrosion model by Zhu-2015, another Mod PCORRC by Zhu in 2018, the Mod LPC model, the Ref-B31G model by Abdelghani in 2018.* In order to comparison with the 2nd-G models, LPC and PCORRC are included in Fig. 10. This figure shows that 1) the Zhu-2005 is an upper bound solution, 2) the Ref-B31G is a lower bound solution, and 3) all other models determine comparable results. Two bound models determine two extreme solutions: one is non-conservative, and the other is over-conservative.

Figure 10 compares Mod-LPC with LPC and M-PCORRC with PCORRC. The new model Zhu-2015 is also included in this figure. It is observed that 1) Mod-LPC is shifted up from the LPC in a factor of 1.03, 2) Mod-PCORRC is shifted up from the PCORRC in the same factor of 1.03, and 3) the two modified models are close to Zhu-2015 model. Thus, strain hardening effect is insignificant for X70.

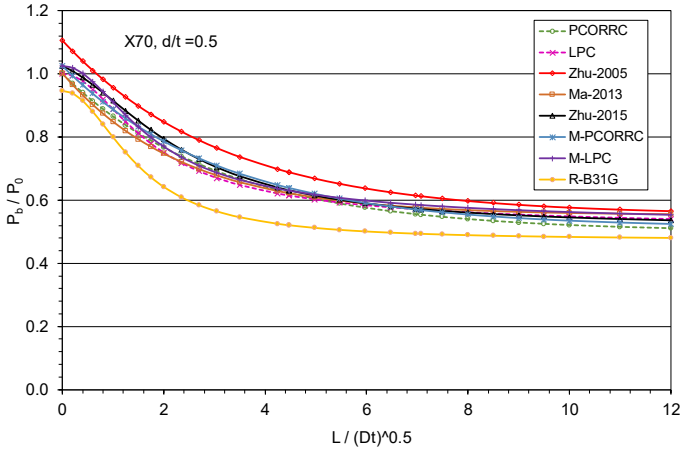

Fig. 9. Comparison of the 3rd-G corrosion models for X70

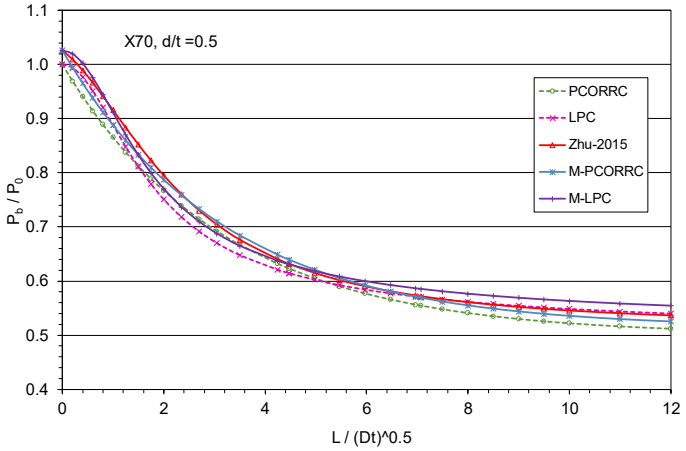

Fig. 10. Comparison of LPC, PCORRC and their modified models for X70

3.4. Validation of corrosion assessment models

3.4.1. Evaluation of the first two generation models

The first two generation models are frequently used in the integrity assessment of aging pipelines. To better understand the difference of available models, the PHMSA office in the U.S. DOT sponsored a large project [55] in the mid-2000s to thoroughly evaluate those corrosion models. A large integrated test database that contains 313 full-scale vessel and ring expansion test data for real and machined metal-loss defects were collected for line pipes ranging from Grade A25 to X100. These experimental tests were conducted by many organizations over more than fifty years in the oil and gas industry. The metal-loss defects were axially isolated, only internal pressure was applied with known pipe geometries, defect sizes, and material properties. Actual material properties were used as needed in the calculations of failure pressure.

Comparisons [58] showed that (1) the RSTRENG model is the most accurate one with the least scatter, and most data points fall into a relatively small scatter; (2) the B31G model is the most conservative one with a large scatter range; (3) the Mod B31G is less conservative than the B31G with a reduced scatter range; and (4) the LPC and PCORRC models predict comparable results with a scatter range similar to the Mod B31G. Note that the two 2nd-G models were developed for defects with uniform bottom, but not for actual river-bottom corrosion defects. Thus, their predictions are conservative. However, the pipeline industry has not accepted the 2nd-G models of LPC or PCORRC models for predicting the remaining strength of actual corrosion defects, and continues to use ASME B31G, or Mod B31G, or RSTRENG in the daily pipeline integrity assessment. On this basis, a decision is made for corroded pipelines if they need a repair, replacement or rerun without an action.

3.4.2. Experimental validation of all three generation models

Kim et al. [47] conducted a set of full-scale experimental tests for machined metal-loss defects and obtained reliable burst pressure data for a Korean X65 pipeline steel. The burst pressure data were reported for machined defects with a fixed uniform depth of d/t=0.5 and six lengths of L=50, 100, 200, 300, 600, and 900 mm. The pipe diameter is 762 mm (30 in.) and the wall thickness is 17.5 mm (0.69 in.). The actual YS and UTS of the X65 pipe are 495 MPa and 565 MPa. The burst pressures are predicted using all 3rd-G corrosion models, and compared with test data, as shown in Figs 11(a) and 11(b).

Figure 11(a) compares the full-scale test (FST) data with predictions from all models: four 1st-G models (B31G, Mod B31G, RSTRENG, and CSA Z662), two 2nd-G models (LPC and PCORRC), and six 3rd-G models (Mod-LPC, Mod-PCORRC, Zhu-2005, Ma-2013, Zhu-2015, and Ref-B31G). For the 1st-G models, 1) the RSTRENG predicts conservative results for all defects, 2) the Mod B31G predictions are very accurate for short defects but non-conservative for long defects with length $L>\sqrt{(20Dt)}$, 3) the B31G predictions are conservative, particularly for long defects, and 4) the CSA Z662 predictions are the lower bound and too conservative.

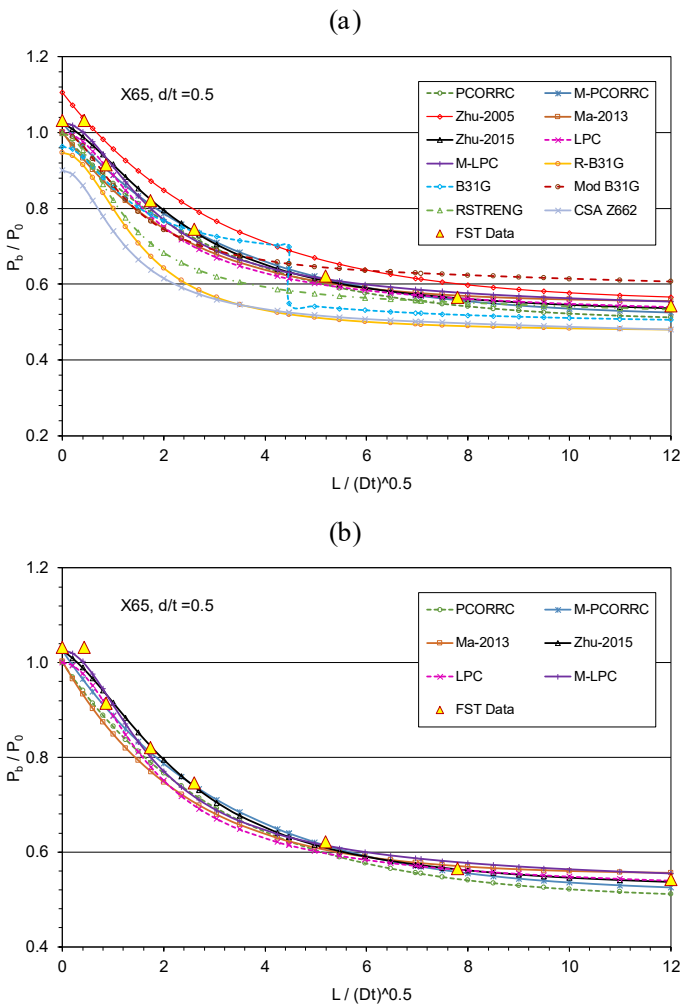

Fig. 11. Comparison of corrosion model predictions with test data, (a) all models, and (b) selected 2nd-G models

For the 2nd-G models, the LPC and PCORRC predictions are comparable and match with the test data in a small conservative error. For the 3rd-G models, 1) the Zhu-2005 model is non-conservative, 2) the Ref-B31G model is too conservative, and 3) all other four models are comparable for all defects.

Figure 11(b) compares the four selected 3rd-G models and the two 2nd-G models with the experimental data. Again, all those six models predict comparable results and closely match the test data. However, further observation shows that 1) PCORRC is slightly conservative for all defects, 2) LPC is conservative for short defects, 3) Ma-2013 is conservative for short defects and slightly non-conservative for long defects, 4) Mod-LPC is accurate for short defects and slightly non-conservative for long defects, and 5) *Zhu-2015 and Mod-PCORRC are nearly identical to each other and the most accurate in comparison to the full-scale test data.*

3.4.3. Experimental validation of Ma-2013 model

Ma et al. [56] collected 79 full-scale experimental data for corrosion defects in pipelines from public literature. The pipeline

grades ranging from X42 to X100 were categorized into three groups, i.e., low strength steels (X42 to X56), mid-strength steels (X60 and X65) and high-strength steels (X80 to X100). Those authors compared their model (Ma-2013) predictions with the full-scale burst data, as shown in Fig. 12, and concluded that the Ma-2013 model is very accurate for the high-strength and mid-strength steels, but less accurate for the low-strength steels.

Recall that the 3rd-G models of Mod-PCORRC, Mod-LPC and Zhu-2015 are comparable to the Ma-2013 model. Thus, it is reasonably anticipated that all these 3rd-G models are accurate to predict burst pressures at least for corrosion defects in the high-strength and mid-strength pipeline steels.

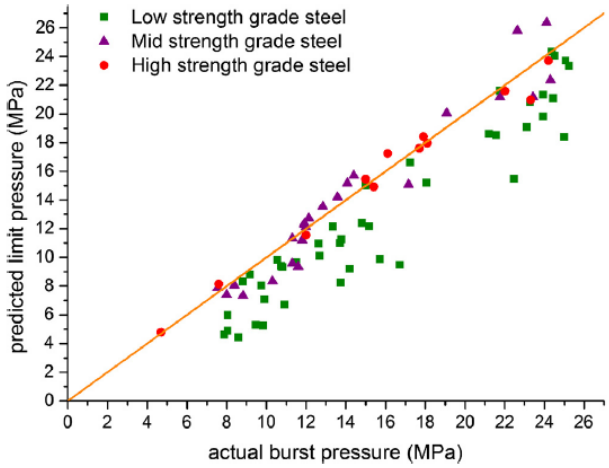

Fig. 12. Comparison of Ma-2013 predictions with full-scale burst data of burst pressure of defects in various pipeline grades [56]

3.4.4. Experimental validation of Mod-PCORRC model

More recently, Leis [60] assessed the reference stress and the geometric term of the PCORRC model and its modified or reformulated version using full-scale experimental datasets for machined defects with flat bottoms for a range of pipeline grades from X52 to X100. Figure 13 compares the predicted failure pressure using the Mod-PCORRC model in Eq. (30) with the actual failure pressure for the machined defects. As evident in this figure, the predictions agree well with the actual data in a very high best-fitting correlation factor of 0.991 between the model predictions and actual data of burst pressure.

Similarly, Leis [60] also evaluated the Mod-PCORRC model using the calibration database of ASME B31G and Mod B31G for a set of complex actual corrosion defects that have irregular river-bottom shapes. The comparison showed a good agreement between the predicted failure pressure and the actual failure pressure with a best-fitting correlation factor of 0.922. In contrast to this, the corresponding best-fitting correlation factor is 0.617 and 0.698, respectively for B31G and Mod B31G. Therefore, those full-scale burst data validate the accuracy of the proposed Mod-PCORRC model, and this model is adequate to use for more accurately predicting the burst pressure of metal-loss defects in pipelines.

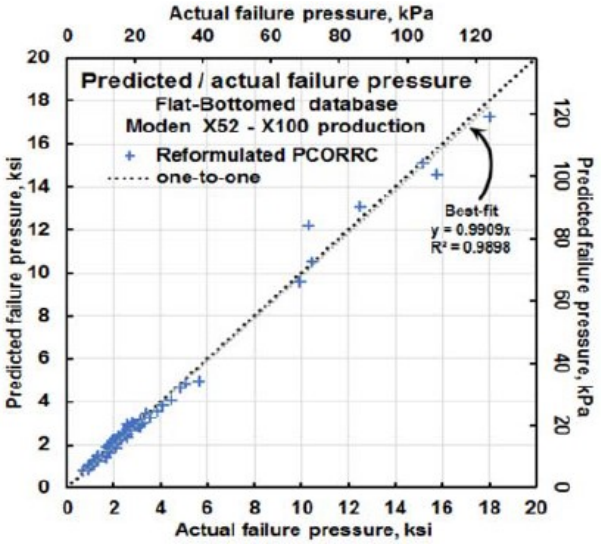

Fig. 13. Comparison of the M-PCORRC predictions with the experimental data for machined defects in modern pipeline grades ranging X52 to X100 [60]

4. Recent progresses

4.1. Thick-wall burst pressure solutions

The thick-wall theory discussed in Section 2.3 for defect-free pipes can be simply extended to corroded thick-wall pipes. Using the Zhu-Leis solution in Eq. (10) for thick walls, Mod-PCORRC model in Eq. (30), Mod-LPC model in Eq. (31) and the new polynomial corrosion model in Eq. (35) are adapted as the 4th-generation for corroded thick-wall pipes, respectively:

$$p_b = 2\left(\frac{2+\sqrt{3}}{4\sqrt{3}}\right)^{n+1}\sigma_{uts}\,ln\left(\frac{D_0}{D_i}\right)\left(1-\frac{d}{t}\left(1-exp\left(-\frac{0.157L}{\sqrt{D(t-d)/2}}\right)\right)\right) \quad (36)$$

$$p_b = 2\left(\frac{2+\sqrt{3}}{4\sqrt{3}}\right)^{n+1}\sigma_{uts}ln\left(\frac{D_0}{D_i}\right)\left[\frac{1-d/t}{1-d/Qt}\right] \quad (37)$$

$$P_b = 2\left(\frac{2+\sqrt{3}}{4\sqrt{3}}\right)^{n+1}\sigma_{uts}ln\left(\frac{D_0}{D_i}\right)\left[1-\frac{d}{t}\left(1-1/\left(1+0.1385\frac{L}{\sqrt{Dt}}+0.1357\left(\frac{L}{\sqrt{Dt}}\right)^2\right)\right)\right] \quad (38)$$

These thick-wall corrosion models should have the similar accuracy to the corresponding thin-wall corrosion models in Eqs (30), (31) and (35) for thin-wall pipes, but much higher accuracy for corroded thick-wall pipes. Experimental valuations of these thick-wall models will not be reported here due to space limit.

4.2. Machine learning models of burst pressure

Recall that Section 2.4 applied the machine learning to model the burst pressure of defect-free pipes. Similarly, ANNs can be employed to model the remaining strength of corroded

pipelines. All ANN approaches used for defect-free pipes are applicable to corroded pipes in the same manner. The only difference is that more input variables and hidden neurons are needed for modeling corroded pipes.

Figure 14 shows the sketch of a typical ANN model for determining burst pressure of corroded pipelines. At least, there will be six input variables: UTS, n, D/t, d/t, L/√(Dt), and W/D, and one output variable: burst pressure. For assumed hidden neurons and hidden layers, the best ANN model can be solved for a giving training dataset and a giving testing dataset. The example of ANN model will be presented elsewhere.

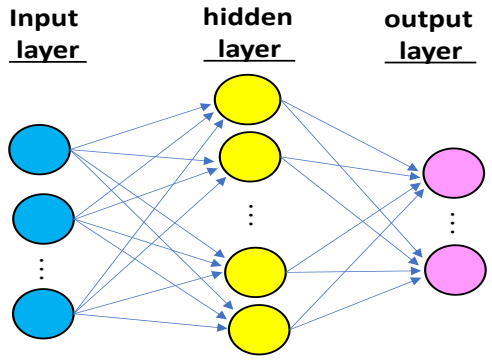

Figure 14. Sketch of typical ANN model for corroded pipes

4.3. PRCI Research on Corrosion Assessment

Corrosion assessment has been one of the major research topics at PRCI for managing pipeline integrity over a half century. Since the early 2000s, the first author has participated in a series of PRCI corrosion projects from EC-2-5 to EC-2-10.

- Project EC-2-5 [61] completed in 2011 assessed the corrosion severity for high-strength pipeline steels.
- Project EC-2-6 [62] completed in 2017 developed a more accurate reference stress for corrosion assessment by using Zhu-Leis flow solution [21] for defect-free pipes.
- Project EC-2-7 Phase I [63] completed in 2016 numerically assessed the PRCI corrosion model errors. Project EC-2-7 Phase II [64] completed in 2017 carried out full-scale tests on machined metal-loss defects to assess corrosion model error for X70 pipes. The FEA results and test data achieved for this project were presented by Leis et al. [17, 65].
- Project EC-2-8 [66] completed in 2019 assessed the applicability of existing metal-loss models for corroded pipelines in low-hardening steels.
- Project EC-2-9 [67] completed in 2019 provided a technical review of the plausible profiles (Psqr) corrosion model that was recently developed at TC Energy [68]. Psqr proposed multiple plausible profiles to use RSTRENG to determine a minimum failure pressure. This approach reduces the conservatism and improves the accuracy of RSTRENG.
- Most recently, Project EC-2-10 Phase I [69] completed in 2020 numerically quantified the defect width effect on the burst failure of metal-loss defects.

Based on the FEA results obtained for EC-2-7 and the reference stress obtained for EC-2-6, an alternative corrosion assessment model was developed, where the bulging factor is a combined function of defect length, depth and width that is different from the original bulging factor. This is a significant improvement. Figure 15 compares the EC-2-6 model with RSTRENG, PCORRC and Mod-PCORRC in reference to the model predictions with the full-scale burst data [47]. It shows that EC-2-6 model is comparable to PCORRC or Mod-PCORRC and improves RSTRENG on the burst pressure prediction.

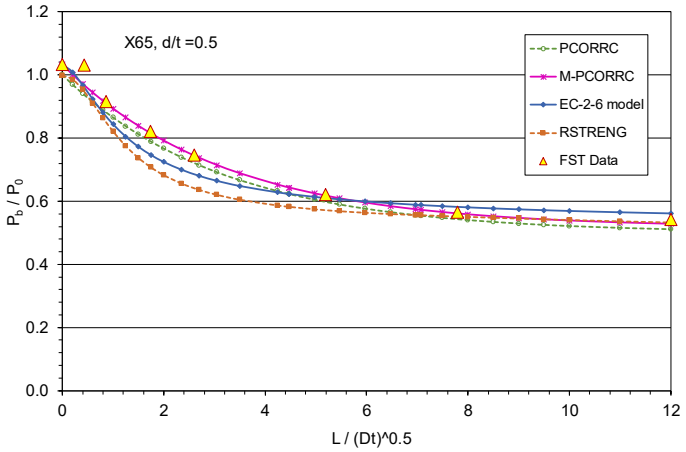

Figure 15. Comparison of burst pressure predicted from four corrosion models with burst test data

4.4. Constraint effect

As well known, the crack-tip constraint due to crack depth and crack length has a significant effect on fracture toughness of surface cracks in ductile steels. Likely, corrosion defect sizes (depth, length and width) have a constraint effect [70] on the remaining strength of defects in ductile pipeline steels. Recently, Zhu [58] numerically explored the constraint effect on the material strength local to metal-loss defect due to defect geometry change. Their results showed that local bulging occurs at a defect and increases with defect length or depth, which is consistent with experimental observations. Because of bulging, larger radial displacement was generated at the defect center, and higher burst stress was resulted correspondingly. Moreover, the Mises stress normalized by the UTS is a function of defect sizes rather than a constant. Clearly, this demonstrates the constraint effect on the local strength of corroded pipeline steels. Such a constraint effect can be calibrated using reliable full-scale burst test data for a well-designed set of defect sizes.

4.5. Bulging factor and shape factor

The conservative corrosion assessment models: ASME B31G, or Mod B31G or RSTRENG remains in use in the oil and gas industry, and thus it is necessary to assess these model errors. A general format [61-63] of B31G criterion can be expressed for the hoop stress at failure S_f, in the form of:

$$S_f = S_R \left[\frac{1 - SF\left(\frac{d}{t}\right)}{1 - SF\left(\frac{d}{t}\right)/BF} \right] \tag{36}$$

where SF denotes shape factor, and BF denotes bulging factor. In B31G, SF=2/3, and BF is given in Eq. (12). In Mod B31G, SF=0.85, and BF is given in Eq. (14). To improve B31G, a general function of three parameters S_R, SF and BF needs to be determined. More recently, Leis et al. [25] discussed the effect of SF and BF on the errors of B31G and Mod B31G models.

For a machined defect with uniform bottom, SF=1, and BF is an undetermined parameter. Recently, the numerical study [17] showed that the BF is a function of both defect length and depth, and the BF of B31G is overestimated for all depths. This is the root cause of conservatism of B31G and Mod B31G.

4.6. Defect width effect

In all corrosion models discussed above, the defect width is not considered because its effect is insignificant generally for non-wide defects. Although the corrosion width is not a primary parameter, but it does affect the burst failure of wide defects. As shown in the PRCI report [69], PCORRC may underestimate the burst pressure for narrow defects (i.e., defect width angle is less than 5°), and overestimate burst pressure for wider defects (i.e., defect width angle is larger than 30°). The width effect has been coupled in the BF of the EC-2-6 model.

5. Major technical challenges

5.1. Experimental burst tests

Full-scale experimental tests play a dispensable role in measurement of reliable burst pressure data. Most full-scale burst tests are conducted using hydrostatic tests that are usually expensive, particularly for large diameter pipes due to material and specimen manufacture costs. To reduce material costs, investigators may use a short cylindrical vessel with a length about two times diameter or even shorter. As a result, test data obtained from a short vessel may be inaccurate and incapable to represent a long pipe, because its burst pressure is likely elevated due to the end-cap effect. This is particularly true for a short vessel with a long defect. Thus, a short vessel should not be used to measure burst pressure in a full-scale test. In general, a test vessel should have at least five times diameter to avoid the end-cap effect. A three-segment design of long pressure vessel is a way to compromise the full-scale test challenge [58].

5.2. Numerical simulation and material failure criteria

The FEA numerical simulation of pipeline failure is based on the continuum theory. However, the continuum theory has no material failure criteria, and thus a prescribed material failure criterion is needed in the FEA simulation to determine material failure local to a defect. Actually, different failure criteria have been used in the FEA calculations of failure pressure, which resulted in different predictions. The most often used material failure criteria in the defect failure simulation includes the RIKS instability model for determining global failure and many local failure criteria, such as the von Mises effective stress equals to 0.9 true UTS, 1.0 true UTS and 1.0 engineering UTS. Thus, use of an appropriate material failure criterion in the FEA is a great challenge, see more detailed discussions by Zhu [58].

5.3. Assessment of real corrosion defects

Assessing real metal loss defects faces many challenges. First is to detect defects in pipelines and to characterize defect sizes. This needs advanced in-line inspection (ILI) technology and tools, such as magnetic flux leakage (MFL), ultrasonic technology (UT), geometric tool and others. Once a corrosion defect is detected and characterized, its assessment is a great challenge. Any real corrosion defect is not an isolated single uniform defect, but a cluster of corrosion pits with a river bottom profile and may be not axially oriented. In addition, separate corrosion clusters may have an interaction to each other, and assessing corrosion defect interaction is another challenge. For some old pipelines, material properties may not be documented for all pipe segments. This can be an additional challenge for assessing corrosion defects in ageing pipelines.

6. Conclusions

This paper delivered a technical review on progress and development of corrosion assessment models for predicting the remaining strength of corroded line pipes. Detailed comparisons and critical evaluations were performed on typical corrosion models for both defect-free and corroded line pipes.

For defect-free pipes, a brief review was made on both the strength and flow theory-based solutions for predicting the burst pressure of thin-wall pipes. Experimental comparisons were presented to validate the Zhu-Leis flow solution. To determine more accurate burst pressure for thick-wall pipes, the newly proposed thick-wall flow solutions and machine learning models were also discussed and validated in comparison to full-scale burst data for a wide range of pipeline grades from GrB to X120. Total 10 models were evaluated for defect-free pipes.

For corroded pipes, available corrosion assessment models were categorized into three generations in terms of the reference stress used in each model. The 1st, 2nd, or 3rd generation was defined when the flow stress, the UTS, or both the UTS and strain hardening rate were used. Total seventeen corrosion models were discussed and evaluated. Of which, five models are the 1st generation, five models are the 2nd generation, and seven models are the 3rd generation. The focus of this work was on two newly proposed models, i.e., Mod-PCORRC and Zhu-2015. Comparisons with full-scale burst data showed that these new corrosion assessment models are more accurate in prediction of remaining strength of corroded pipelines.

In addition to the three generation models, this work also introduced three typical thick-wall corrosion models and machine learning models as the 4th generation for predicting more accurate burst pressure for corroded thick-wall pipelines. Moreover, recent progresses on improving corrosion models were reported, including the PRCI corrosion research projects, constraint effect, bulging factor, and defect width effect. Finally, major technical challenges facing the corrosion model development were discussed, including full-scale experiments, numerical simulation, material failure criteria, and real corrosion defect assessment. It is anticipated that the 4th-generation models will become the efficient tools for real corrosion assessment.

ACKNOWLEDGEMENTS

The first author is grateful to Dr. Brain Leis for his technical supports & discussions on PRCI projects over the past 20 years.

This work was supported by the Laboratory Directed Research and Development (LDRD) program within the Savannah River National Laboratory (SRNL). This document was prepared in conjunction with work accomplished under Contract No. 89303321CEM000080 with the U.S. Department of Energy (DOE) Office of Environmental Management (EM).

References

[1] US DOT PHMSA, Pipeline Incident 20 Year Trends, *www.phmsa.dot.gov/data-and-statistics/pipeline*, 2018.

[2] Dai L, Wang D, Wang T. Analysis and comparison of long-distance pipeline failures, *J Petroleum Eng*, 2017; 2017: 3174636.

[3] Ossai CL, Boswell, B. Davies IJ, Pipeline failure in corrosive environments – A conceptual analysis of trends and effects, *Engng Fail Anal*, 53; 2015: 36-58.

[4] Zhu XK. Strength criteria versus plastic flow criteria used in pressure vessel design and analysis, *J Press Vessel Technol*, 138 (2016) 041402.

[5] Christopher T, Sarma BS, Potti PK. A comparative study on failure pressure estimation of unflawed cylindrical vessels, *Int J Press Vessels Pip*, 79 (2002) 53-66.

[6] Law M, Bowie G. Prediction of failure strain and burst pressure in high yield-to-tensile strength ratio line pipes, *Int J Press Vessels Pip*, 84 (2007) 487-492.

[7] Zhu XK, Leis BN. Evaluation of burst pressure prediction models for line pipes, *Int J Press Vessels Pip*, 89 (2012) 85-97.

[8] Keifner JF, Atterbury TJ, Investigation of the behavior of corroded line pipe, Project 216 Interim Report, February 1971.

[9] Maxey WA, Kiefner JF, Eiber RJ, Duffy AR. Ductile fracture initiation, propagation and arrest in cylindrical vessels, *Fracture Toughness*, ASTM STP 514, Part II, 1972, pp. 347-362.

[10] Kiefner JF, Maxey WA, Eiber RJ, Duffy AR. Failure stress levels of flaws in pressurized cylinders, *Progress in Flaw Growth and Fracture Toughness Testing, ASTM STP 536*, American Society for Testing and Materials, 1973, pp. 461-481.

[11] ASME B31G-2009, *Manual for Determining the Remaining Strength of Corroded Pipelines*, American Society of Mechanical Engineers, New York, USA, 2009.

[12] Cosham A, Hopkins P, Macdonald KA. Best practice for the assessment of defects in pipelines, *Engng Fail Analy*, 14, (2007) 1245-1265.

[13] BS 7910:2013 + A1:2015, *Incorporating Corrigenda Nos. 1 and 2 Guide on Methods for Accessing the Acceptability of Flaws in Metallic Structures*, British Standards Institution, London, UK, 2015.

[14] API 579-1/ASME FFS-1, *Fitness for Service*, Third Edition, June 2016.

[15] Zhu XK, Assessment methods and technical challenges of remaining strength for corrosion defects in pipelines, *Proceedings of the ASME Pressure Vessels and Piping Conference*, Prague, Czech, July 15-20, 2018.

[16] Zhu XK, A new material failure criterion for numerical simulation of burst pressure of corrosion defects in pipelines, *Proceedings of the ASME pressure vessels and Piping Conference*, Boston, Massachusetts, USA, July 19-23, 2015.

[17] Leis BN, Zhu XK, Orth F, Aguiar D, Perry L. Minimize model uncertainty in current corrosion assessment criteria, *PRCI-APGA-EPRG 21th Joint Technical Meeting on Pipeline Research*, Colorado Springs, Colorado, USA, May 1-5, 2017

[18] Zhou W, Huang GX. Model error assessments of burst capacity models for corroded pipelines, *Int J Press Vessels Pip*, 99-100; 2012: 1-8.

[19] Amaya-Gomez R, et al. Reliability assessments of corroded pipelines based on internal pressure – A review, *Eng Fail Anal*, 98; 2019, 190-214.

[20] Bhardwaj U, Teixeira AP, Soares CG. Uncertainty quantification of burst pressure models of corroded pipelines, *Int J Press Vessels Pip*, 188; 2020: 104208.

[21] Zhu XK, Leis BN. Average shear stress yield criterion and its application to plastic collapse analysis of pipelines, *Int J Press Vessels Pip*, 83; 2006: 663-671.

[22] Zhu XK, Leis BN. Accurate prediction of burst pressure for line pipes, *J Pipeline Integrity*, 4; 2004: 195-206.

[23] Zhu XK, Leis BN, Influence of yield-to-tensile strength ratio on failure assessment of corroded pipelines. *J Press Vessel Technol,* 127; 2005: 436-442.

[24] Seghier MEAB, Keshtegar B, Elahmoune B. Reliability analysis of low, mid and high-grade strength corroded pipes based on plastic flow theory using adaptive nonlinear conjugate map, *Eng Fail Anal*, 90; 2018: 245-261.

[25] Zimmermann S, Marewski U, Hohler S, Burst pressure of flawless pipes, *3R Inter*, Special Edition, 46; 2007: 28-33.

[26] Zimmermann S, Hohler S, Marewski U. Modeling of ultimate limit states: Burst pressure and circumferential elongation of flawless pipe, *APRA-EPRG-PRCI 16th Biennial Pipeline Research Joint Technical Meeting*, Australia, April 2007.

[27] Zhou W, Huang T. Model error assessment of burst capacity models for defect-free pipes, *Proceedings of International Pipeline Conference*, 2012, Calgary, Canada, Sept 25-28.

[28] Bony M, Alamilla JL, Vai R, Flores E. Failure pressure in corroded pipelines based on equivalent solutions for undamaged pipe, *J Press Vessel Technol*, 132; 2010: 051001.

[29] Lyons CJ, Race JM, Chang E, Cosham A, Wetenhall B, Barnett J. Validation of the NG-18 Equations for thick-walled pipelines, *Eng Fail Analy*, 112; 2020: 104494.

[30] Zhu XK, Wiersma B, Sindelar R, Johnson WR. "New Strength Theory and Its Application to Determine Burst Pressure of Thick-Wall Pressure Vessels," *Proceedings of the ASME 2022 Pressure Vessels and Piping Conference*, July 17-22, 2022, Las Vegas, Nevada, USA. PVP2022-84902.

[31] Zhu XK, Johnson WR, Sindelar R, Wiersma B. "Machine Learning Models of Burst Strength for Defect-Free Pipelines," *Proceedings of the ASME 2022 Pressure Vessels and Piping Conference*, July 17-22, 2022, Las Vegas, Nevada, USA. PVP2022-84908.

[32] API Specification 5L, Lin Pipe, the 46th Edition, American Petroleum Institute, April 2018.

[33] Folias ES. An axial crack in a pressured cylindrical shell, *Int J Fract Mech*, 1; 1965: 104-113.

[34] Coulson K.W, Worthingham RG. Standard damage assessment approach is overly conservative, *Oil and Gas J*, April 9, 1990.

[35] Kiefner JF, Vieth PH. *A Modified Criterion for Evaluating the Remaining Strength of Corroded Pipe*, Final report on Project PR 3-805 to the Pipeline Research Committee of the American Gas Association, 1989.

[36] Kiefner JF, Vieth PH, Roytman I. Continuing validation of RSTRENG, Pipeline Research Supervisory Committee, A.G.A Catalogue No. L51689, December 1996.

[37] Ma B, Shuai J, et al. Analysis on the latest assessment criteria of ASME B31G-2009 for the remaining strength of corroded pipelines, *J Fail Anal Prevention*, 11; 2011: 666-667.
[38] Ritchie D, Last S. Shell 92 – Burst criteria of corroded pipelines – defect acceptance criteria, *EPRG-PRCI 10th Biannual Joint Technical Meeting on Pipeline Research*, Cambridge, UK, 1995.
[39] CSA Z662-19, *Oil and Gas Pipeline Systems*, Canadian Standards Association, Mississauga, Canada, 2019.
[40] Fu B and Kirkwood MG, Determination of failure pressure of corroded linepipes using nonlinear finite element method, *Proceedings of the 2nd International Pipeline Technology Conference*, Vol.II, 1995, pp. 1-9.
[41] Fu B, Batte AD. New methods for assessing the remaining strength of corroded pipelines, *EPRG/PRCI 12th Biennial Joint Technical Meeting on Pipeline Research*, Groningen, The Netherlands, 1999, Paper 28.
[42] Det Norske Veritas, *Recommended Practice DNV-RP-F101 – Corroded Pipelines,* 2015.
[43] Leis BN, Stephens DR, An alternative approach to assess the integrity of corroded line pipes – Part I: current status and Part II: alternative criterion, *Proceedings of the Seventh International Offshore and Polar Engineering Conference*, Honolulu, Hawaii, USA, May 25-30, 1997.
[44] Stephens DR, Leis BN. Development of an alternative criterion for residual strength of corrosion defects in moderate-to-high toughness pipe, *Proceedings of International Pipeline Conference*, Calgary, Canada, Oct 1-5, 2000.
[45] Choi JB, Goo BK, Kim JC, et al. Development of limit load solutions for corroded gas pipelines, *Int J Press Vessels Pip*, 80; 2003: 121-128.
[46] Yeom KJ, Lee YK, OH KH, Kim WS. Integrity assessment of a corroded API X70 pipe with a single defect by burst pressure analysis, *Eng Fail Anal*, 57; 2015: 553-561.
[47] Kim WS, Kim YP, Kho YT, Choi JB. Full scale burst test and finite element analysis on corroded gas pipeline, *Proceedings of the fourth International Pipeline Conference*, Calgary, Alberta, Canada, Sept 30 – Oct 3, 2002.
[48] Benjamin AC, Andrade EQ. Modified method for the assessment of the remaining strength of corroded pipelines, *Proceedings of 2003 Rio Pipeline Conference*, Rio, Brazil, October 22-24, 2003.
[49] Souza RD, et al., Rupture tests of pipeline segments containing long real corrosion defects, *Experimental Techn*, 31; 2007: 46-51.
[50] Zhu XK. Leis BN, Theoretical and numerical predictions of burst pressure of pipelines, J Press Vessel Technol, 129; 2007: 644-652.
[51] Besel M, S. Zimmerman S, et al. Corrosion assessment method validation for high-grade line pipe, *Proceeding of the 8th International Pipeline Conference*, Calgary, Alberta, Canada, Sept 27 – Oct 1, 2010.
[52] Chiodo MSG, Ruggieri C. Failure assessments of corroded pipelines with axial defects using stress-based criteria: numerical studies and verification analyses, *Int J Press Vessels Pip*, 86; 2009: 164-176.
[53] Zhu XK, Corrosion assessment methods for pipelines with long blunt defects, *J Pipeline Engng*, 14; 2015: 111-120.
[54] Noronha DB, Benjamin AC, Andrade EQ. Finite element models for the prediction of the failure pressure of pipelines with long corrosion defects, *Proceedings of the 4th International Pipeline Conference*, Calgary, Canada, Sept 29 – Oct 3, 2002.
[55] Chauhan V, Brister J. *A review of methods for assessing the remaining strength of corroded pipelines*, US DOT Final Report 153A, November 2009.
[56] Ma B, Shuai J, Liu D, Xu K. Assessment on failure pressure of high strength pipeline with corrosion defects, *Eng Fail Anal*, 32; 2013: 209-219.
[57] Zhu XK. Burst failure models and their predictions of buried pipelines, *Proceedings of the Conference on Asset Integrity Management – Pipeline Integrity Management under Geohazard Conditions*, Houston, TX, USA, March 25-28, 2019.
[58] Zhu, XK. A Comparative Study of Burst Failure Models for Assessing Remaining Strength of Corroded Pipelines, *J Pipeline Sci and Engng*, 2021, 1: 36-50.
[59] Abdelghani M, et al., Prediction of the rupture pressure of transmission pipelines with corrosion defects, *J Press Vessel Technol*, 140; 2018: 041701.
[60] Leis BN. Continuing Development of Metal-Loss Severity Criteria – Including Width Effects, *Proceedings of the ASME International Pipeline Conference*, Calgary, AB, Canada, Sept 28 - Oct 2, 2020.
[61] Leis BN, Zhu XK. *Assessing Corrosion Severity for High-Strength Steels*, PRCI Project Report for EC-2-5, Catalog No. PR003-103603-R01, March 2013.
[62] Leis BN, Zhu XK, T McGaughy T. *Reference Stress for Metal-Loss Assessment of Pipeline*, PRCI Project Report for EC-2-6, Catalog No. PR185-173600, December 2017.
[63] Leis BN, Zhu XK, McGaughy T. *Assessment of Corrosion Model Error for Metal-Loss Defects in Pipelines*, Phase I of PRCI Project Report for EC-2-7, Catalog No. PR185-143600, December 2016.
[64] Orth F, Zhu XK, McGaughy T, Leis BN. *Assessment of Corrosion Model Error for Metal-Loss Defects in Pipelines: Phase II – Full-Scale Experiments*, PRCI Project Report for EC-2-7, Catalog No. PR185-163609, December 2017.
[65] Leis BN, Zhu XK, et al., *Step improvement in metal-loss assessment criteria for pipelines*, APGA-EPRG-PRCI 22nd Joint Technical Meeting on Pipeline Research, Brisbane, Australia, 29 April - 3 May 2019.
[66] Leis BN, Zhu XK, McGaughy T., *Applicability of Existing Metal-Loss Criteria for Low-Hardening Steels*, Catalog No. PRCI Project Report for EC-2-8, PR185-173611, December 2019.
[67] Kiefner J. Peer review of the plausible profiles (Psqr) Corrosion assessment model, PRCI Project Report for EC-2-9, PR-218-183607, September 2019.
[68] Zhang S, et al., A more accurate and precise method for large metal loss corrosion assessment, *Proceedings of the ASME International Pipeline Conference*, Calgary, Canada, Sept 24 - 28, 2018.
[69] Zhu XK, McGaughy T. *Development of a Comprehensive Metal-Loss Assessment Criterion – Phase I on Quantify Defect Width Effect on Failure of Metal-Loss Defects*, PRCI Project Report for EC-2-10, Catalog No. PR185-193601-R01, June 2020.
[70] B.N. Leis, X.K. Zhu, Corrosion Assessment Criteria: Rationalizing Their Use for Vintage vs Modern Pipelines, DOT Research and Special Projects Agency, DTRS56-03-T-0014, September 2005.